We are IntechOpen, the world's leading publisher of Open Access books Built by scientists, for scientists

4,800
Open access books available

122,000
International authors and editors

135M
Downloads

Our authors are among the

154
Countries delivered to

TOP 1%
most cited scientists

12.2%
Contributors from top 500 universities

CLARIVATE ANALYTICS BOOK CITATION INDEX INDEXED

WEB OF SCIENCE™

Selection of our books indexed in the Book Citation Index in Web of Science™ Core Collection (BKCI)

Interested in publishing with us?
Contact book.department@intechopen.com

Numbers displayed above are based on latest data collected.
For more information visit www.intechopen.com

Chapter 2

A Modern Philosophy for Creep Lifing in Engineering Alloys

Mark Whittaker, Veronica Gray and William Harrison

Additional information is available at the end of the chapter

http://dx.doi.org/10.5772/intechopen.71829

Abstract

Lifing of components which are likely to be subject to high temperature creep deformation is a critical area to a range of industries, particularly power generation and aerospace. In particular, extrapolation of short term data to predict long-term allowable creep stresses is an area of significant importance, since no appropriate method of accelerating tests has been discovered. Traditional methods for extrapolation are mainly based around power law type equations that have historically formed the basis of creep mechanism understanding. The current chapter however, seeks to offer alternative approaches in the field, particularly emphasising the need to link lifing approaches to observable micro-mechanical behaviour.

Keywords: creep, Wilshire equations, dislocations, region splitting

1. Introduction

The following Chapter is dedicated to the late Brian 'George' Wilshire, a large, unforgettable and missed presence in the field of creep.

Creep is a time dependant process of deformation that affects materials operating under stress and temperature. This elongation of material which can occur at in-service stresses and temperatures means that design engineers needs to consider this dynamic process, otherwise risk catastrophic and possibly fatal failure. A specific case which requires consideration is the power generation industry which requires long design lives that are often extended to over 30 years or over 250,000 h [1]. This chapter discusses issues with reference to specific materials used in power generation and extends the approaches to the aerospace nickel superalloy Waspaloy. It should be noted the issues discussed here are relevant to all engineering materials that experience creep.

Initially defined as a field of study in the late 1940s via publication of the first test standards [2–5], creep and the methods used to predict it are a relatively new field of study. As such, forming the backbone of almost all methods to predict creep are power-law derived relationships that use the dependency of $\acute{\varepsilon}_m$ and t_f on σ, with equations of the form:

$$M/t_f = \acute{\varepsilon}_m = A\sigma^n \, exp\,(-Q_c/RT) \tag{1}$$

Using this relationship the values of A, stress exponent n, and activation energy Q_c vary with test conditions. Examining this relationship it is comprised of three empirical components:

$$M = \acute{\varepsilon}_m \, t_f \tag{2}$$

$$\acute{\varepsilon}_m \, \alpha \, \sigma^n \tag{3}$$

$$\acute{\varepsilon}_m \, \alpha \, exp\,(-Q_c/RT) \tag{4}$$

These components are Eq. 2, which is the Monkman-Grant relationship, stating that the product of the minimum creep rate and time to failure equals a constant, M [6]. Eq. 3 is Norton's law which relates minimum creep rate to stress through the exponent n [7]. Lastly, Eq. 4 is the Arrhenius relationship which is an empirical description of reaction rates, particularly for diffusion in chemistry [8]. From these relationships we see M, n, and Q_c are defined as constants over a stress and temperature range associated with a creep mechanism. Changes in these values should reflect a change in creep mechanism and signal a new creep regime ultimately affecting the prediction made using Eq. 1. Furthermore, within this equation there is the ability to infer the creep mechanism. The activation energy, Q_c, described by the Arrhenius component provides a measure of energy within the system that can be linked with activation energies for mechanisms such as diffusion [8]. The power-law also has traditionally linked the value of n to mechanisms through some first principles derivation, but mostly is reliant on empirical evidence [7].

1.1. Power-law creep mechanisms

The power-law equations were derived to describe creep deformation behaviour based upon secondary, or steady-state creep being present in the creep curve. However, detailed inspection of normal creep strain/time curves show that a minimum creep rate, $\acute{\varepsilon}_{m,}$ not a steady-state value is usually reached where the decaying primary rate is offset by the tertiary acceleration as seen in **Figure 1**. Rather than seeking to identify *'steady-state'* mechanisms, emphasis should therefore be directed to the deformation processes governing strain accumulation and the various damage mechanisms causing the creep rate to accelerate, leading to eventual fracture [9].

Power-law approaches are based on having n and Q_c characterise the creep mechanism which raises issues when applied to high performance materials such as those used in gas turbines and power generation. To begin with, it is necessary to consider the power-law in Eq. 1, where n and Q_c are derived from different empirical relationships to represent the same physical

http://dx.doi.org/10.5772/intechopen.71829

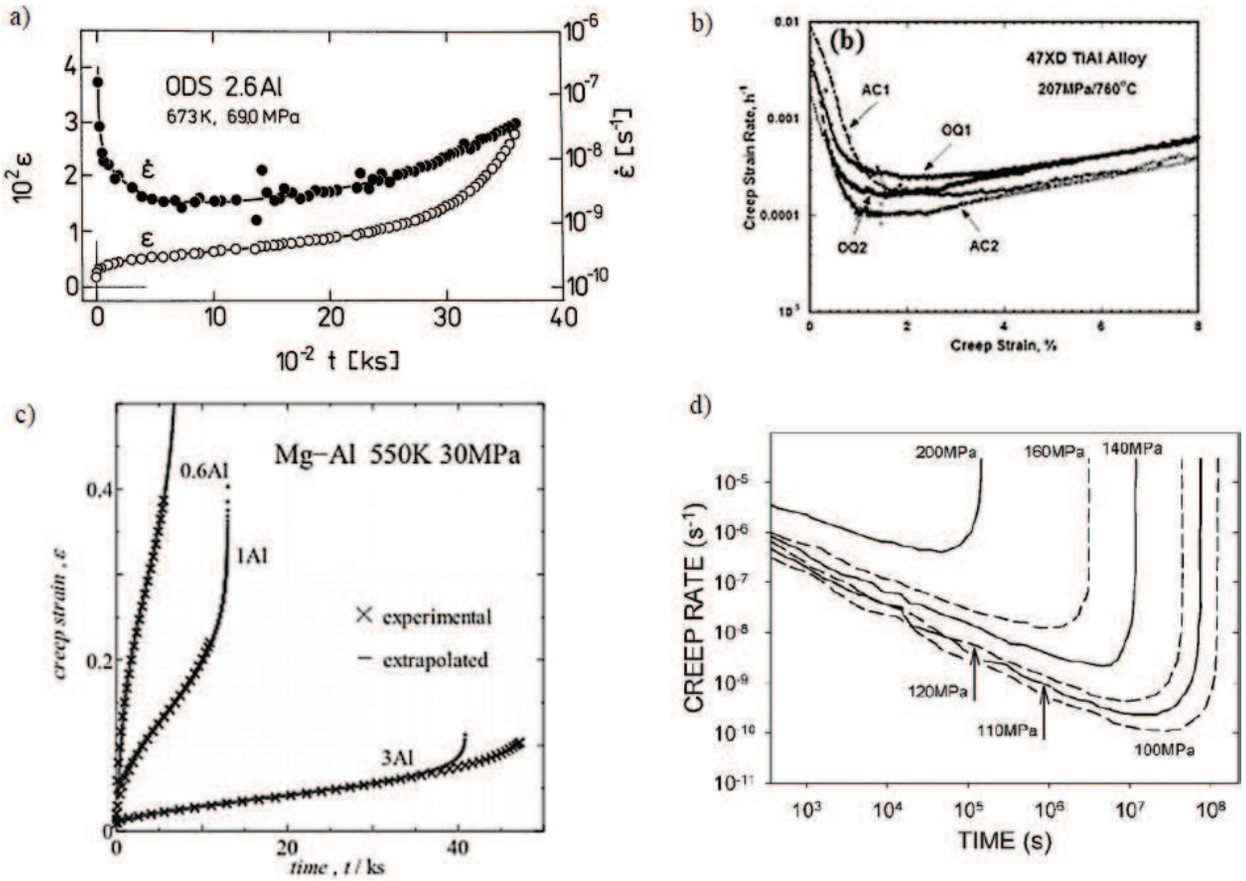

Figure 1. Examples of minimum creep rate, rather than secondary or steady-state creep for (a) aluminium alloy [10], (b) TiAl alloy [11], (c) MG-Al alloy [12], and (d) grade 91 steel [13].

process i.e. a creep mechanism. Activation energy or Q_c is a numerical value obtained from the application of the Arrhenius equation where the gradient of $\acute{\varepsilon}_m$ vs. $1/T$ for a given stress should yield a constant for the same creep mechanism. The value of Q_c is then also comparable to physically derived known quantities such as the activation energies of specific diffusion processes. The changing value of Q_c with regards to Eq. 1 should produce *'regions'* where expected creep life behaviour changes with creep mechanism.

Considering the stress exponent, n, its definition and application is even less physically reliable. The stress exponent n can be derived from first principles for very limited and specific cases such as those for ice derived in the 1950s [14–18]. From specific derivation a value of $n = 1$ is associated with diffusion whilst n = 4–7 is considered to indicate dislocation creep mechanisms [19]. The actual meaning of n is material dependant and often requires significant microstructural investigation and understanding. Beyond this, if n is an indicator of creep mechanism then it should act similarly to Q_c. In other words, n should remain constant for the stress-temperature range where a specific creep mechanism is dominant then transition to a different appropriate constant value when the mechanism changes. Indeed, n is only seen to remain constant over limited stress-temperature ranges then become non-constant, known as Power-Law Breakdown [19].

Values derived from Eq.1 should allow inference of the underlying creep mechanism. It is useful to compare studies of similar material datasets in order to consider the effectiveness of the technique and the consistency of its application:

- For Grade 122 steel, using the data provided by NIMS [20] several analyses have been conducted [21]. One analysis saw a decrease of $n \approx 16$ to $n \approx 5$ when the temperature of the tests increased from 823 to 1023°K with Q_c varying from 680 to 500 kJ/mol [22]. Another analysis [20, 23] for the same steel saw a high stress regime with $n \approx 60$ and $Q_c = 1045$ kJ/mol, and a low stress regime at $n \approx 5$ and $Q_c = 640$ kJ/mol.
- For Grade 91 steel, the stress exponent ranges from $n > 16$ to $n \approx 4$ with $Q_c = 400–780$ kJ/mol [24].
- Seen also in Grade 92, $n \approx 18$ drops to $n \approx 3$ and $Q_c = 540–760$ kJ/mol over the test range [25].
- In Grade 23 $n \approx 13$ at high stress and drops to $n \approx 6$ at low stresses whilst $Q_c = 300–535$ kJ/mol [26]

When considering these results, the combination of n and Q_c values do not produce consistency and indeed show themselves to highly dependent on their application, with the value of Q_c particularly showing a significant stress dependency. It is also extremely difficult to align the values gained out of the analyses of these typical engineering materials with the values proposed by traditional theory.

1.2. Power-law constants

One of the backbones of creating reliable modelling is reproducibility. In terms of n and Q_c it has already been shown that for the case of Grade 122, interpretation by those conducting the analysis can produce widely differing results. Considering the power-law based equations used to predict creep properties the use of a Time–Temperature Parameter (TTP) is often employed. The TTP is derived from $log(t_f)$ vs. $1/T$ (or T in some cases) where the gradient, and/or intercept are used to define the relationship.

For the Larson-Miller approach [27], a graph of $log(t_f)$ vs. $1/T$ is made where the gradient is the Larson-Miller Parameter, P_{LM}, and the intercept at $1/T \sim 0$ is the Larson-Miller Constant, C_{LM}. These TTPs are then related to stress via:

$$P_{LM} = f(\sigma) = T\left(C_{LM} + log\left(t_f\right)\right) \tag{5}$$

This means to use this equation, values for P_{LM} are mapped against stress and a function chosen. A similar process is conducted for a variety of methods including Orr et al. [28], Manson and Succop [29], Manson and Haferd [30], and Goldhoff-Sherby [31] which each offer differences in curve shape. Additionally, these methods offer different approaches to activation energy:

- Larson-Miller: P_{LM} is equivalent to Q_c determined by mapping $log(t_f)$ vs. $1/T$ at constant stress. From Eq. 5, P_{LM} and therefore Q_c is expected to vary with stress in a continuous manner rather than step change with creep mechanism.
- Goldhoff-Sherby: PGS is also equivalent to Qc but requires the linear fit of $log(tf)$ vs. $1/T$ at constant stress to converge ensuring that Qc cannot be constant.
- Orr-Sherby-Dorn: COSD is equivalent Qc but is constrained to be constant.

A description of these methods, their implementation and efficacy can be found in [32, 33].

In considering these power-law derived methods that implement a TTP, there are issues ensuring reproducibility and physical accuracy. During the implementation of the aforementioned creep models, a parameter is mapped in terms of stress e.g. P_{LM} vs. σ. Consequently a function is chosen to describe this relationship. The definition of this function is not in a fixed form and therefore each implementation of the power-law based relationships is subject to *'user'* preference/choice. This is especially problematic when extrapolating as the functions chosen to represent stress dependency can produce unphysical results and therefore be extremely subjective and unreliable when extrapolating beyond the sampled test data.

1.3. Power-law summary

Power law based equations form the basis of almost all creep modelling approaches used today. Its underlying principles are a unification of the Monkman-Grant, Norton, and Arrhenius relationships into an empirical equation. As creep has advanced as a field and included more extreme conditions and high performance materials, the power-law has struggled to keep up with the array of mechanisms. From the power-law's application to steel, its inability to deal with these mechanisms through the combination of the activation and stress exponent terms, Q_c and n, is clear. Furthermore the application of power-law based models often requires users to choose the TTP-stress relationship introducing 'bespoke' modelling unique to the persons/group that have performed it. In identifying the weaknesses of the power-law, this chapter looks at the work of Wilshire and colleagues in their attempt to address some of these issues.

2. The Wilshire approach

The last 70 years of creep has been reliant on using power-law based analysis and stems from the widely held assumption that dislocation creep mechanisms are dominant at high stresses, with transition to diffusion based creep mechanisms at low temperatures. For pure aluminium, pure copper and the precipitate hardened Al7010, Wilshire and Whittaker [9], examined the creep curve beyond the *'steady-state'* to identify the dominant creep mechanisms.

For the precipitate hardened alloy Al7010, the role of diffusional creep in low stress regimes assumed by the power-law was challenged. For this material, precipitate-free zones sometimes found in the vicinity of grain boundaries in the low stress regime increased in width with increasing test duration, offering preferred locations for dislocation movement. This suggests the low stress behaviour of Al7010, and indeed other precipitate hardened materials, is not solely diffusional creep as assumed previously, thus leading to the work by Wilshire to develop a new approach to creep lifing. These mechanisms should be therefore supported and reflected in the value of the activation energy which can be derived either from the time to failure, t_f, or the minimum creep rate, $\dot{\varepsilon}_m$ with respect to *1/T*.

Considering the power-law approach to creep modelling a number of issues have been highlighted which need to be addressed. Seeing the issues facing the field of creep and its inability to unite results with microstructural processes, Wilshire[1] and colleagues proposed an alternative to the power-law.

2.1. An alternative to power-law based equations

Utilising the power-law and its Arrhenius basis, the activation energy is calculated at constant stress. For a creep mechanism to occur it requires a certain amount of energy known as activation energy. For a creep test, kinetic energy is created by applying a stress and thermal energy by applying temperature. This energy is used by the system to activate creep mechanisms. From the Arrhenius or power-law approach it assumes that the dominant energy process or mechanism is determined by the absolute kinetic energy and therefore measures activation energy at constant stress.

Unlike a chemical or gaseous system, a solid has limitations where the maximum thermal energy is 0-T_m°K and the maximum kinetic energy of the system is 0-σ_{UTS} MPa.[2] Using this idea, the temperature dependant UTS provides the upper limit of a solid system in terms of both kinetic and thermal energy. To implement this idea the stress is normalised such that:

$$M/t_f = \dot{\varepsilon}_m = A^* \left(\frac{\sigma}{\sigma_{UTS}}\right)^n exp\left(-Q_c^*/RT\right) \tag{6}$$

It should be noted in Eq. 6 that $A \neq A^*$, and $Q_c \neq Q_c^*$. In chemistry terms, both Q_c and Q_c^* are apparent activation energies rather than true activation energies. By definition true activation energy is a chemical or thermal reaction rate derived from first principles for a mechanism [34]. Apparent activation energy is the reaction rate that is dependent on a time to failure or a cumulative reaction process such as $\dot{\varepsilon}_m$. The minimum creep rate, $\dot{\varepsilon}_m$, is often used instead of t_f due to it being less sensitive to failure mechanisms and anomalies, but it is still is a time dependant cumulative value and as such produces an apparent activation energy.

[1] Wilshire is used as an abbreviation for Wilshire and colleagues. We recognise research is collaborative, but for simplicity we use Wilshire to represent all those involved in developing this work. Collaborators can be found in the references at the end of the chapter.

[2] When referred to in this work, the Ultimate Tensile Stress, UTS or σ_{UTS} is always temperature dependant.

The existing literature often uses minimum creep rate, $\dot{\varepsilon}_m$, and secondary creep rate, $\dot{\varepsilon}_s$, interchangeably, however as previously shown in **Figure 1** a secondary phase does not exist for many materials under a range of conditions and is not reliably observed in test data [35]. Therefore rather than seeking to identify *'steady-state'* creep mechanisms, the focus of the Wilshire approach is directed at the deformation processes that define strain accumulation, and the damage mechanisms that accumulate and lead to eventual failure [9]. This allows a minimum creep rate to be defined as a decaying primary rate is offset by tertiary acceleration.

From Eq. 6, the normalisation of the stress means that the normalised activation energy, Q_c^*, is evaluated at on a relative scale. This reflects the physical limitation of the system such that the material at its UTS will undergo failure no matter the specific amount of stress or temperature applied. The approach promotes the idea that a solid system has a maximum energy state, and that systems in the same relative energy should be experiencing the same mechanism. To evaluate Q_c^*, the gradient of $log(t_f)$ vs. $1/T$ is evaluated at constant normalised stress i.e. constant σ/σ_{UTS}, or, using regression analysis fitting Q_c^* from $ln(-ln(\sigma/\sigma_{UTS}))$ vs. $ln(t_f\ exp.(-Q_c^*/RT))$. It should be noted that some initial investigations using this method normalised the test stress by the temperature dependant yield stress rather than the UTS. This normalisation focused on the elastic limit of the material as it is a defined point of mechanism change. If σ_Y/σ_{UTS} remains fairly constant with temperature then activation energy values will be equivalent to conducting normalisation by the UTS.

The goal of creep modelling is to create a relationship where the apparent activation energy is equivalent to the true activation energy of the dominant creep mechanism. From the previous section it can be seen that for the power-law approach, the apparent activation energy ranging up to 1045 kJ/mol does not correlate with the true activation energy of any known creep mechanism. Using a normalised stress approach to calculate Q_c^*, Wilshire found for Grade 91, 92 and 122 that for all these steels $Q_c^* \approx 300$ kJ/mol, equivalent to lattice diffusion for the material [35].

2.2. The Wilshire equations

Although normalising creep test stress has shown to provide more reasonable Q_c^* values, as well as a more consistent relationship between stress and time to failure, it still contains the problematic stress exponent, n. Indeed, Eq. 6 still suffers from the vulnerabilities outlined in §1.1 and 1.2. To deal with n and power-law relationships, Wilshire developed a series of equations:

$$\sigma/_{\sigma_{UTS}} = exp\left\{-k_u\left[t_f \cdot exp\left(-Q_c^*/_{RT}\right)\right]^u\right\} \tag{7}$$

$$\sigma/_{\sigma_{UTS}} = exp\left\{-k_v\left[\dot{\varepsilon}_m \cdot exp\left(-Q_c^*/_{RT}\right)\right]^v\right\} \tag{8}$$

$$\sigma/_{\sigma_{UTS}} = exp\left\{-k_w\left[t_\varepsilon \cdot exp\left(-Q_c^*/_{RT}\right)\right]^w\right\} \tag{9}$$

These equations use the apparent activation energy Q_c^*, evaluated at constant σ/σ_{UTS}. The constants k_u, u, k_v, and v are evaluated at $ln(-ln(\sigma/\sigma_{UTS}))$ vs. $ln(t_f.exp.(-Q_c^*/RT))$, and $ln(-ln(\sigma/\sigma UTS))$ vs. $ln(\dot{\varepsilon}_m.exp.(-Q_c^*/RT))$ respectively. Unlike the power-law, constants in Eqs. 7 and 8

are indeed constant over each creep region and therefore do not require the user to choose relationships between variables. In contrast, Eq. 9 is designed to predict tims to specific strains and can potentially be utilised to model the whole creep curve where k_w and w are functions of strains. This however is not discussed further here as full creep curve modelling is discussed in a separate chapter.

Another important aspect of the Wilshire Equations is incorporation of basic physical limits. As $\dot{\varepsilon}_m \rightarrow 0$, then $t_f \rightarrow \infty$ when $\sigma/\sigma_{UTS} \rightarrow 0$. Also, as $\dot{\varepsilon}_m \rightarrow \infty$, then $t_f \rightarrow 0$ when $\sigma/\sigma_{UTS} \rightarrow 1$. This minimum physical limitation is inherent in the Wilshire equations but not so in the power-law meaning it is possible for the power-law to produce unphysical results.

3. Application of the Wilshire equations

3.1. Yield behaviour of polycrystalline copper

To demonstrate the application of the Wilshire Equations with respect to the power-law, the example of polycrystalline pure copper is first considered [9, 36].

Samples were machined from cold-drawn 10 mm rods of oxygen-free high-conductivity copper i.e. 99.95% wt. Cu. Test pieces had a gauge length of 25 mm and diameter of 4 mm. In order to obtain a grain size of ~40 μm, the test pieces were annealed under a vacuum of 10^{-4} Pa for

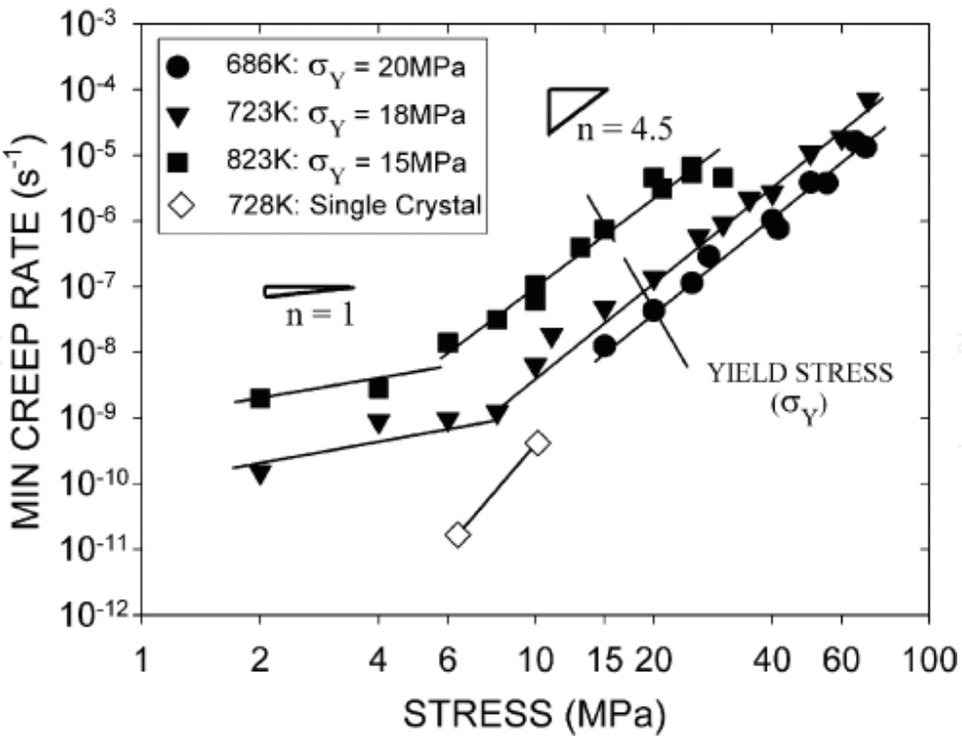

Figure 2. Power-law analysis of polycrystalline copper with n = 1, 4.5 [36].

3600s at 973°K. To ensure no inhomogeneous grain growth, tests were conducted at 686, 723 and 823°K, markedly below the annealing temperature. Upon investigation, no dynamic recrystallization or grain growth was observed under the test stress-temperature combinations used. Tests were conducted on 10:1 constant stress Andrade-Chalmers cam creep machines complying with BS EN 10291:2000.

Conducting power law analysis using the minimum creep rate, $\acute{\varepsilon}_m$, two distinct creep regimes can be observed in **Figure 2** with $n = 1$ and $n = 4.5$ and $Q_c = 110$ kJ/mol. From a classical power-law interpretation, the change in n is consistent with a change from diffusion to dislocation based creep at $\leq 0.61T_m$ and aligns with understood microstructural evolution [37–39]. Immediately from this analysis it was noted that the value of the constant M from Eq. 2 with longer tests and higher temperatures reduces from ~0.07 to ~0.02.

If the normalised power-law in Eq. 6 is applied using an activation energy of 110 kJ/mol, then the relationship between normalised stress, σ/σ_Y, and $t_f.exp(Q_c/RT)$ is approximately linear as seen in **Figure 3**.

Classically the yield strength denotes the transition from elastic to plastic behaviour and as such a change in material behaviour either side would be expected. From power-law analysis there is no indication that creep behaviour changes in the higher stress regime. Looking at the test data in **Figure 4**, the shape of the creep curve changes as test conditions go from above to below yield, σ_Y. With higher temperatures and lower stresses, less primary creep was seen, whilst more tertiary creep is observed, also noting the lack of steady-state creep. Also, with

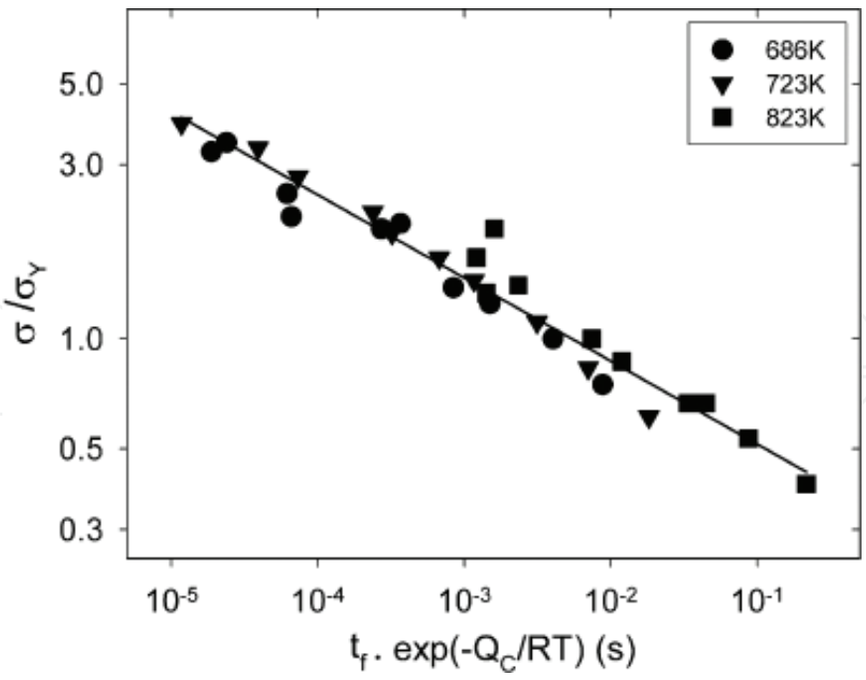

Figure 3. Normalised power-law analysis of polycrystalline copper showing linear trend between normalised stress and time to failure with $Qc = 110$ kJ/mol [36].

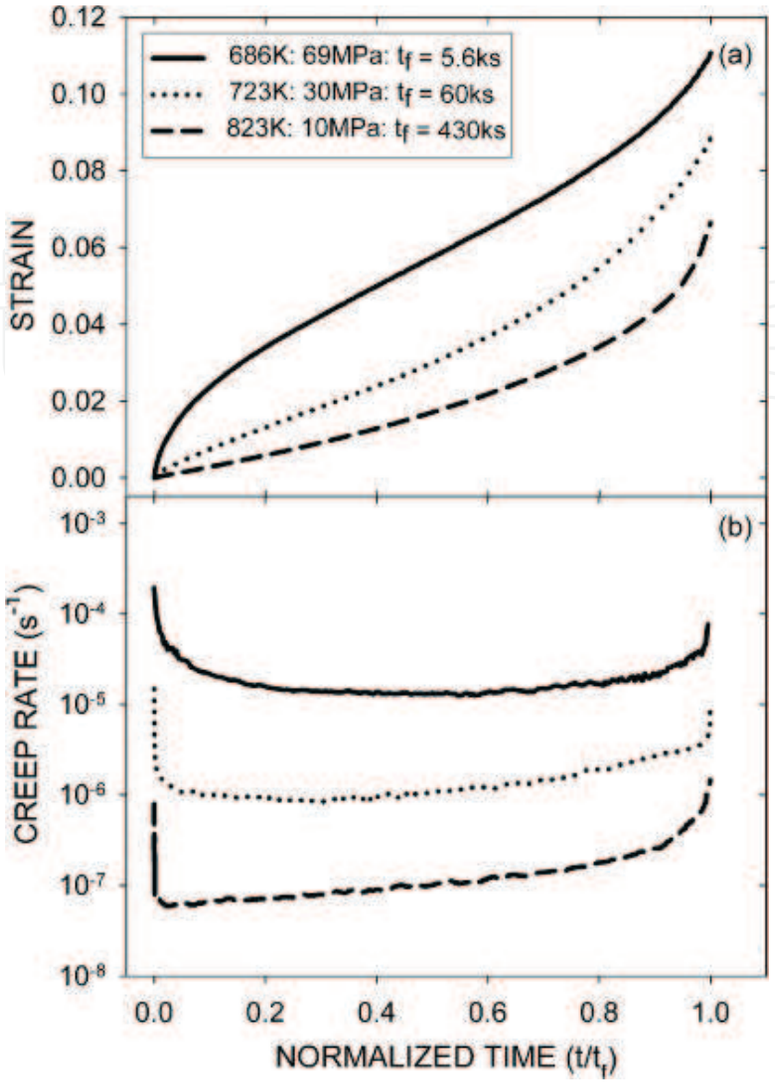

Figure 4. Changing creep curve shape of polycrystalline copper (a) strain vs. normalised time, and (b) creep rate vs. normalised time [36].

increasing test stress the point at which the minimum creep rate reached occurs later in the test. This supports the Wilshire approach of considering creep in terms of primary and tertiary creep rather than steady-state as polycrystalline creep curves transition from primary-dominated to tertiary-dominated curves with increasing temperature and test duration. Furthermore, it suggests in conjunction with other evidence [36], that power-law changes in n are not related to creep mechanism transitions, but rather the complex relationship between changes in $\acute{\varepsilon}_m$ with changing test conditions.

Knowing there is a change in the shape of creep curves as test conditions pass over the yield stress, the equations used to model the data should reflect this transition. From the power-law and normalised power-law we see no indication of a different creep regime around the yield stress. However, by use of the Wilshire approach, the normalised activation energy

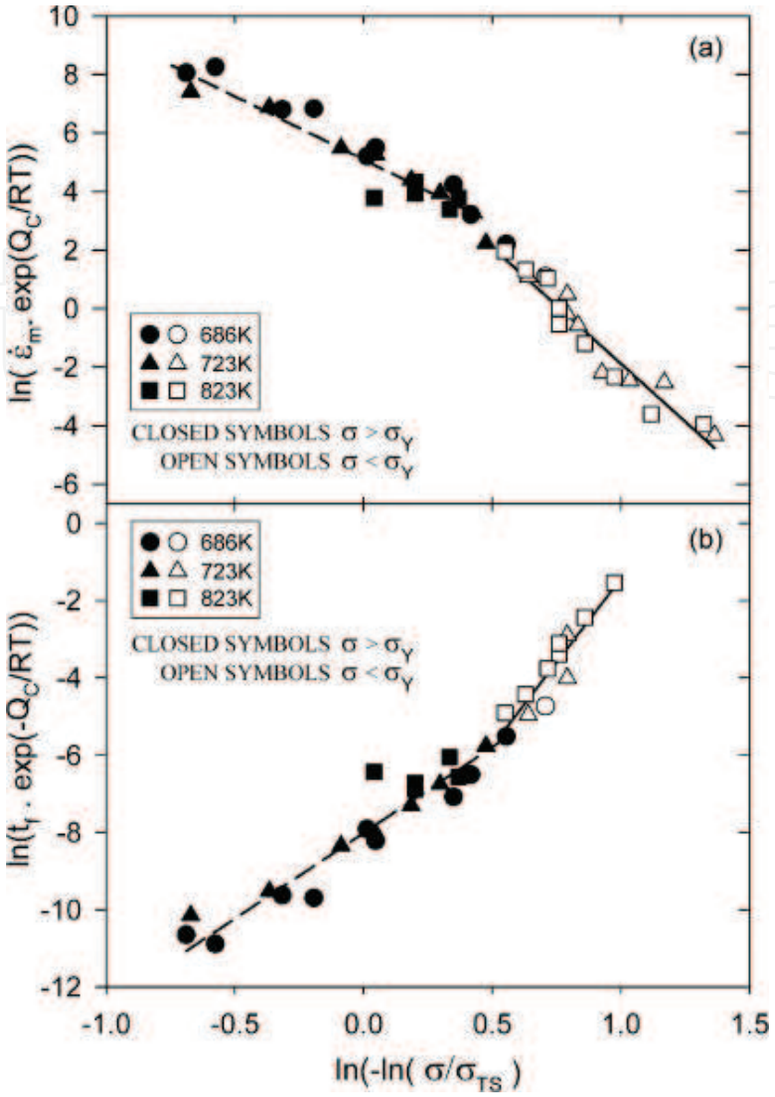

Figure 5. Application of the Wilshire equations to polycrystalline copper demonstrating two regions, above and below yield [36].

was found to be $Q_c^* \approx 110$ kJ/mol which coincides with the associated value for grain boundary diffusion. This mechanism is confirmed by microstructural observations made in Ref. [36]. Implementing Eq. 8, the Wilshire approach shows two linear regions in **Figure 5** when determining k_v and v. Notably results from above yield tests lie in one regime and below yield in another.

In identifying two regimes, the Wilshire Equations are implemented in two regimes, above and below the yield stress. The results are observed in **Figure 6** where the Wilshire approach in comparison to the power-law produces a predictive method that reflects changes in creep mechanism at the yield stress. The power-law on the other hand suffers from changing n and inevitably power-law breakdown without capturing the change in behaviour that occurs at yield.

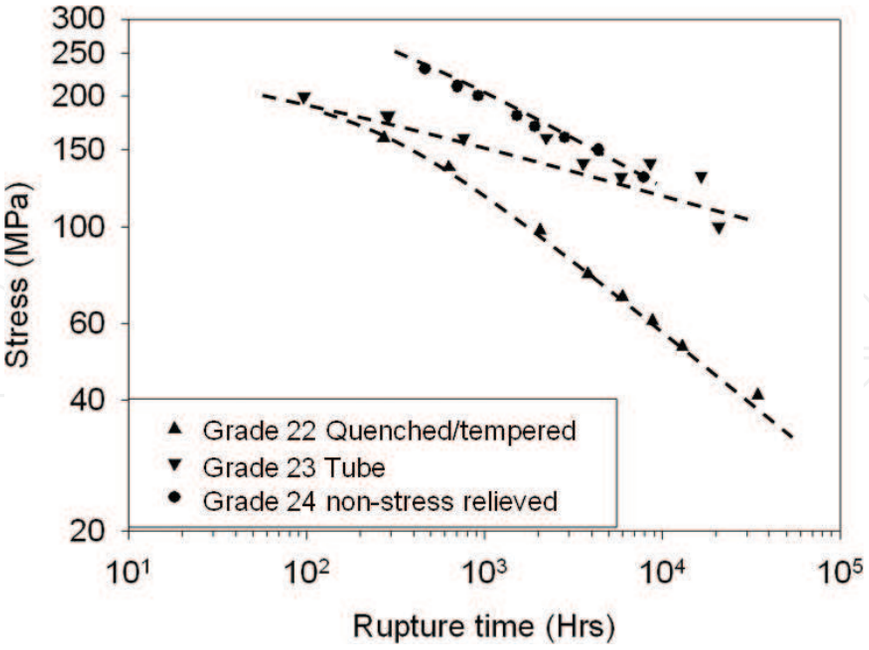

Figure 6. The stress dependence of the creep life at 873 K (600°C) for Gr. 22, 23, and 24 steels [47].

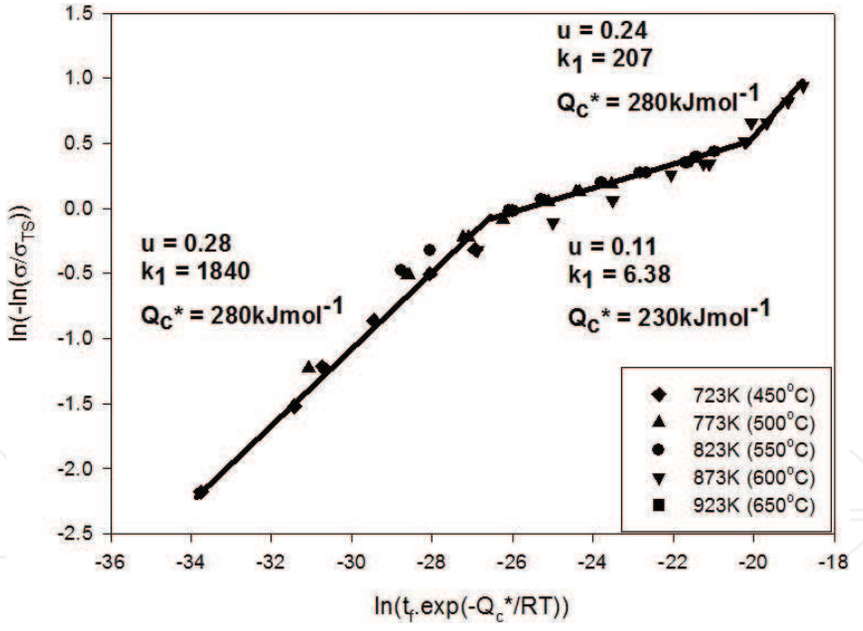

Figure 7. Adopting Eq. 7, k_u, u and Q_c^* values are determined by plotting of $ln[t_f.exp.(-Q_c^*/RT)]$ vs. $ln[-ln(\sigma/\sigma_{UTS})]$, for Gr.22 tube [47].

3.2. Long-term prediction of 9–12% steels

Creep is a significant factor in modern engineering, especially for the power generation industry. Having a design life of over 25 years, power generation relies on extrapolating creep test

data rather than performing costly long-term tests. The need to be able to predict long-term creep behaviour from short term tests is therefore crucial for any creep modelling method to be successful [40].

To design for such a long working life under often non-steady stress and temperature, the benchmark used is nominally the 'allowable tensile creep strengths' [41]. These strengths are 0.67 or 0.8 of the minimum stress causing rupture in 100,000 h or, the stress that results in a creep rate of 0.01% per 1000 h i.e. ~3×10^{-11} s^{-1}. To conduct tests to 100,000 h or ~11 years is unfeasible and therefore short term test data is extrapolated to these values. One group of materials particularly used in this industry is 9–12% Cr steels or Grade 91, 92 and 122. Having undergone these long-term tests, this dataset provided by NIMS [42–44] allows the long-term extrapolation capability of a creep model to be evaluated.

Using the normalised power-law approach of Eq. 6, predicting long-term behaviour of 9–12% Cr steels is problematic. Overall for Grade 91, 92 and 122 the constant M, increases with longer tests. Specifically for Grade 122, Q_c goes from ~500 to 680 kJ/mol with decreasing stress and increasing temperature. Over the same range n falls from ~16 to ~5. These ranges of values are common for high stress tests on alloys strengthened by fine precipitates or insoluble particles [45]. Due to this inconsistency, predicting long-term creep behaviour using the normalised power-law method was abandoned for a parametric power-law approach such as those detailed in §1.2. Due to the problems with these methods discussed in §1.2, these methods are unable to extrapolate long-term data with sufficient accuracy to 100,000 h from 30,000 h tests [46].

It is therefore appropriate to apply the Wilshire Equations to evaluate its ability to predict long-term creep behaviour from short term creep tests. Normalising by σ_{UTS} the activation energy for Grade 91, 92 and 122 was found to be 300 kJ/mol for these martensitic steels. This activation energy is close to that of lattice diffusion in the alloy steel [13]. To test the long-term extrapolation capability of the Wilshire Equations, data from <5000 h and <30,000 h was used. Using Q_c^* = 300 kJ/mol, it was observed that for Grade 92 and 122 there were 2 regions similar to polycrystalline copper, i.e. two linear regimes with different values of k_u and u. Only one region was observed for Grade 91. This can be corroborated with micro-structural behaviour. When examining the Reduction of Area (RoA) with regards to $\acute{\varepsilon}_m$, it was noticed that Grade 92 and 122 displays behaviour consistent with longer duration and higher temperature tests having increasing boundary cavities and thus experiencing a

Temperature	Grade 91	Grade 92	Grade 122
823°K (550°C)	154 (149)	182 (178)	196 (199)
848°K (575°C)	117 (112)	140 (137)	151 (155)
873°K (600°C)	87 (82)	104 (103)	113 (116)
898°K (625°C)	62 (59)	76 (75)	81 (84)
923°K (650°C)	43 (39)	53 (53)	53 (58)

Table 1. Creep rupture strengths (100,000 h) predictions for Grade 91, 92 and 122 from t_f < 30,000 h, and t_f < 5000h (in brackets), MPa [47].

Analysis method	823°K (550°C)	873°K (600°C)	923°K (650°C)
ECCC	166	94	49
Wilshire t_f<30,000 h	154	87	43
Wilshire t_f<5000 h	149	82	39
Tenaris	153	86	46
ECCC-MRM	152	86	44
ECCC-MC	149	84	44
ECCC-LM	157	94	51
ECCC-LM (ed)	150	98	42

Details can be found in [47].

Table 2. Creep rupture strength predictions for a number of methods for comparison.

transition from ductile transgranular to brittle intergranular failure. This was not observed for Grade 91.

The values of k_u and u showed a small variation between the values from tests <30,000 h and those <5000 h. In applying this 2 region approach, it yields creep rupture strengths listed in **Table 1** where it can be seen the extrapolation of creep data from <5000 h tests using the Wilshire approach is almost equivalent to the extrapolations from data <30,000 h.

From **Table 2**, in comparison to other employed extrapolation methods by NIMS, ECCC etc. that use datasets up to <70,000 h, the Wilshire Equations show a remarkable improvement in extrapolation capability. Furthermore, the Wilshire Equations, unlike the other employed methods, reflects the observed change in material ductility thus demonstrating its capability to reflect microstructural and mechanism changes.

Through wider application, the method of implementing the Wilshire equations has evolved especially as demonstrated when applied to the 2.25Cr series of alloys, Grade 22, 23 and 24 [47]. These steels provide a test to the Wilshire equations as Grade 22 (2.25Cr-1Mo) steel has long been utilised and has a wealth of results thanks to NIMS providing both short and long-term data. Furthermore, the development of Grade 23 (2.25Cr-1.6 W) and particularly Grade 24 (2.25Cr-1Mo-0.3 V) steel offers the potential to implement an improved material, if confidence can be provided in predictive methods such as the Wilshire equations.

Initial application of the Wilshire Equations proved difficult, since rather than the two distinct regions seen in previous alloys described above, a third region was observed for longer duration/high temperature tests [47]. Evaluation of test pieces revealed that this behavioural change was most likely due to the degradation of the bainitic microstructure in the material, with the high temperature and long exposure leading to an overaged ferritic microstructure with coarse molybdenum carbide particles also present. In order to provide optimised fits to each of the three materials, the value of the activation energy was allowed to vary in each of

the three regions seen in **Figure 6**. With surprising consistency the Q_c^* value was found to be approximately 280 kJ/mol for tests conducted above the initial yield stress of the material, 230 kJ/mol for the intermediate region, and, 280 kJ/mol for low stress/higher temperature tests [47].

The three regions of seemingly complex behaviour can be rationalised in a manner consistent with the observed microstructural behaviour, as well as elongation and reduction in area measurements. Above the yield stress, creep takes place through the generation and movement of new dislocations, formed at appropriate sources, due to the fact that the yield stress of the material is exceeded. When the applied stress falls below the yield stress, the creep lives become longer than that expected from direct extrapolation of results when $\sigma > \sigma_Y$. This is because grain deformation is restricted, thus creep occurs only by grain boundary zone deformation when $\sigma < \sigma_Y$. A second break occurs in **Figure 6** which is a consequence of the bainite regions in the initial ferrite/bainite microstructure degrading to ferrite and molybdenum carbide particles in long-term tests with very coarse carbides along the grain boundaries. As a result, the creep rates are faster, and the creep lives are significantly shorter than expected by extrapolation of the intermediate stress data when the bainitic microstructures are present [48].

Subsequent application of this varying activation energy was found to improve fits in a range of other materials [49, 50], whilst remaining consistent with the observed micromechanical behaviour.

3.3. Mechanisms of Waspaloy

In an initial investigation of Al7010, Wilshire observed that power-law equations struggle to deal with precipitation strengthened materials [9] due to their inherit assumption of diffusional creep. As such a study was carried out on the nickel superalloy Waspaloy. Details of the material and creep experiments performed can be found in Whittaker et al. [50]. Constant stress creep tests were performed from 550 to 800°C and 140–1150 MPa. From power-law analysis the activation energy at high stresses is ~350 kJ/mol but increases to 700 kJ/mol at low stress with the threshold between high and low stress occurring at ~600 MPa.

Applying the Wilshire Equations, two values of activation energy were observed. For high stress tests, $Q_c^* = 400$ kJ/mol with $k_v = 434$ and $v = -0.24$. For low stress tests $Q_c^* = 340$ kJ/mol with $k_v = 72$ and $v = -0.14$, noting the threshold between the regimes determined from fitting approximately coincides with the yield stress. As with the previous examples, when the creep curve is examined above and below this threshold (yield), the shape of the creep curve goes from primary-dominated to tertiary-dominated (see **Figure 8**).

Rather than relying solely upon creep curve shape, further investigation was conducted in order to verify the creep mechanisms. To do so, a series of creep tests was undertaken at graded levels of stress both above and below the yield stress at a temperature of 700°C. From the starting material, transmission electron microscopy (TEM) in **Figure 9** shows a bimodal distribution of γ' precipitates, with the secondary precipitates approximately 200 nm in

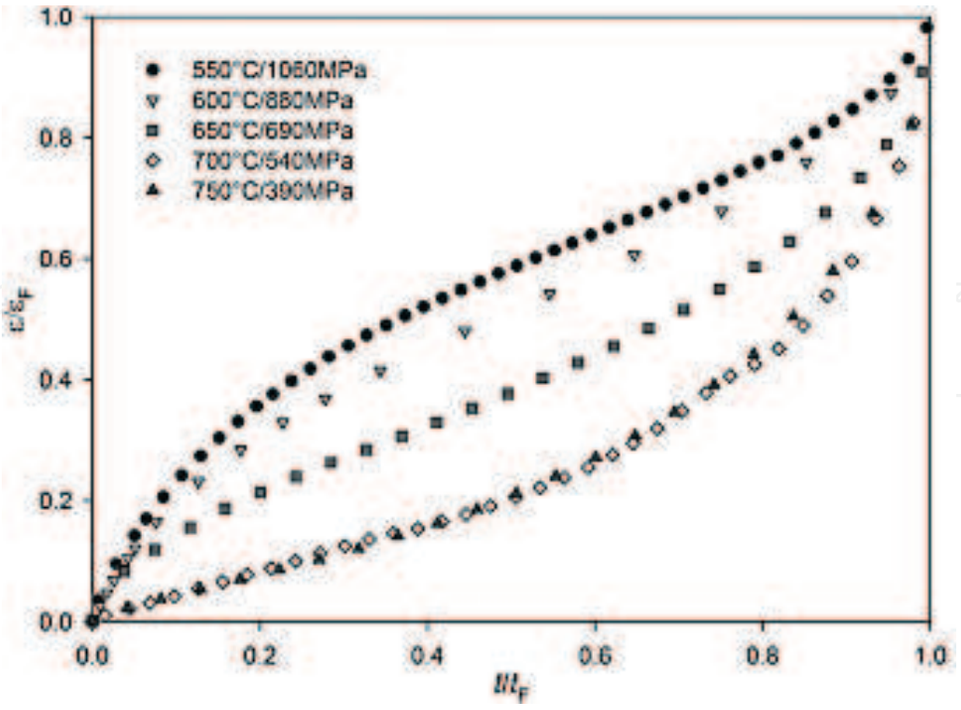

Figure 8. Changing creep curve shape of Waspaloy plotted on a normalised scale [50].

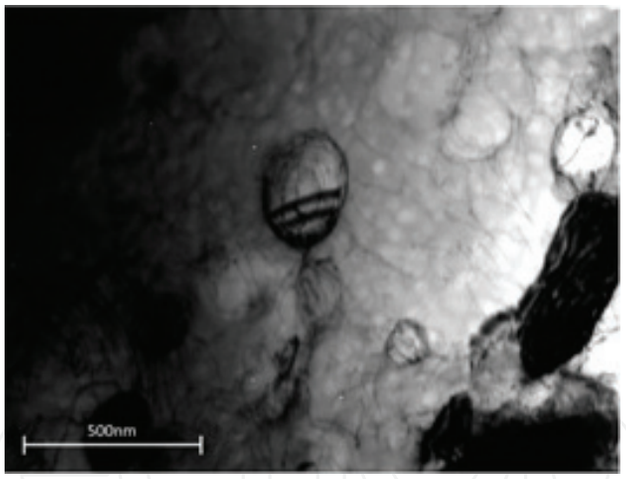

Figure 9. TEM of Waspaloy microstructure in original, un-tested state [50].

diameter and the tertiary of the order of 50 nm diameter. In the γ matrix, dislocations are present in moderate numbers in loose networks that avoid passing through the secondary precipitates. On the grain boundaries some carbides were visible and additionally there was evidence of strain recovery in a series of sub-grains with low angle boundaries.

In order to separate the mechanisms of plasticity from creep, tensile tests to ~0.2% proof stress (740 MPa) at 700°C were examined by TEM, **Figure 10**. It was found that the dislocation

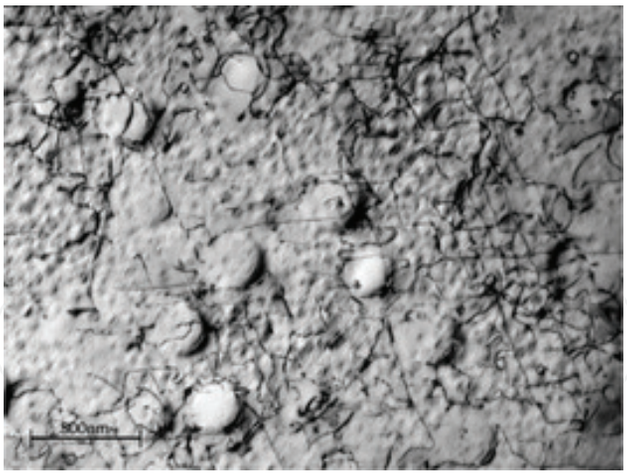

Figure 10. TEM of Waspaloy microstructure after tensile testing [50].

density had increased with most single dislocations cutting through the tertiary γ′, and other dislocations looping around the secondary precipitates. The low angle sub-grains in the tensile sample were the same as those observed in the virgin material.

To investigate creep mechanisms, creep tests were performed at 500, 600, 700 and 800 MPa at 700°C and interrupted once the minimum creep rate was reached. The test pieces were air cooled under reduced load and then prepared for TEM. In **Figure 11a**, at 500 MPa there is a low dislocation density where the dislocations Orowan loop around the secondary γ′, but also the tertiary γ′ which was observed to have the occasional stacking fault. The sub-grains at the boundaries also exhibited this dislocation behaviour.

For specimens crept at 600 MPa and 700 MPa there is a change in behaviour to that seen at 500 MPa. In **Figure 10b** for 600 MPa, noting a reduction in Orowan looping, the dislocation density has increased and stacking faults in the secondary and tertiary γ′ are evident as precipitates are cut by superlattice partial dislocations. From these stacking faults, slip is occurring on more than one slip plane. Although the dislocation spacing between precipitates is increased compared to 500 MPa, it is still below the tertiary precipitate spacing thus indicating the main impediment to slip is the tertiary precipitates. Looking at the grain boundaries, low angle sub-grain are still present but now have a sub-structure which is a combination of dislocation recovery and strain hardening processes.

At above yield conditions of 800 MPa the dislocation density of the material is extremely high to the point where individual dislocations are difficult to identify. This is seen in **Figure 11c**, where the dislocations are extremely dense but mostly confined to the γ and the tertiary γ′ with occasional stacking faults in the secondary γ′. The larger precipitates even in above yield conditions, continue to resist cutting by lattice dislocations.

From this investigation it can be seen that there is a change in dislocation behaviour above and below yield. Below the yield stress, dislocation densities are relatively low and increase

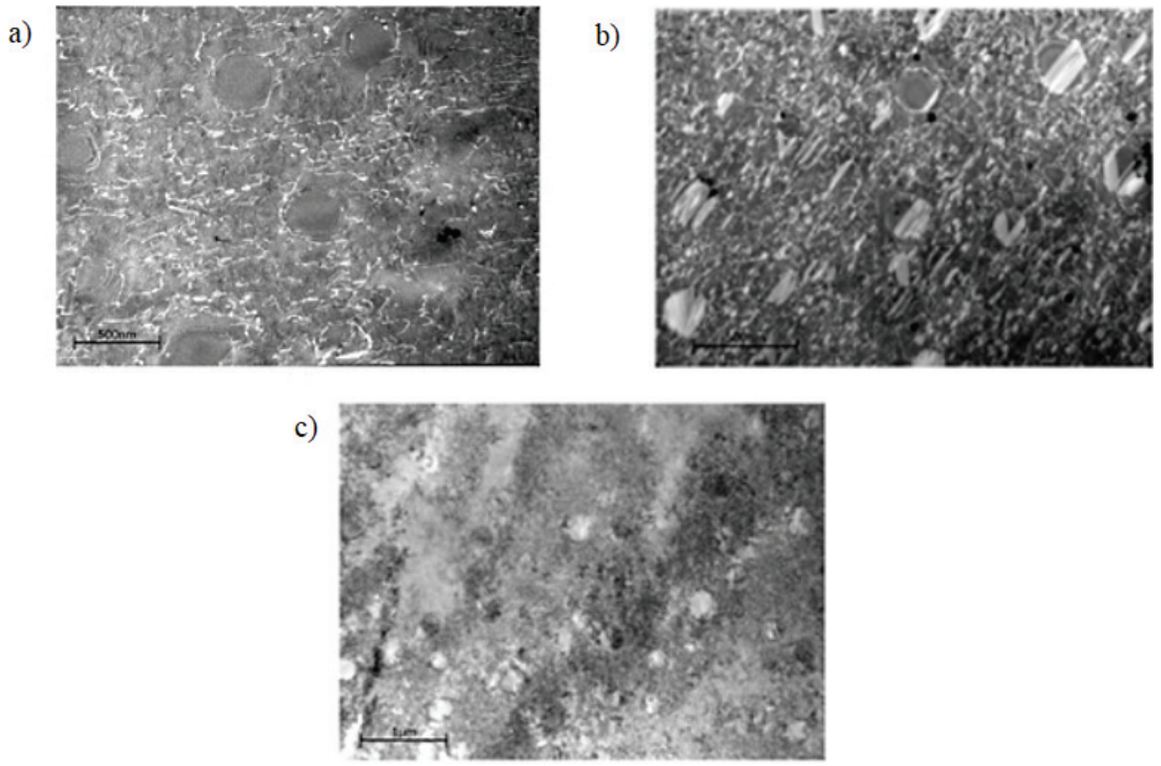

Figure 11. TEM of Waspaloy microstructure after creep at 700°C at (a) 500 MPa, (b) 600 MPa, and (c) 800 MPa [50].

slightly with stress with the sub-grains at the boundaries fairly unaffected. Above the yield point, dislocation density increases to the point where the dislocation spacing is closer than that of the precipitates and the sub-grain structure around the grain boundaries is obliterated by the increase in dislocations throughout. This is interpreted as below yield creep being controlled by dislocation climb around tertiary γ′ precipitates. Above yield creep is controlled by the climb and recovery of dislocation tangles. When considered in light of the Wilshire Equations, the change in activation energy at approximately yield from 340 to 400 kJ/mol reflects this change in mechanism.

4. Region splitting

Having a method of analysing creep data that reflects actual microstructural or mechanism change is crucial to advance the field of creep. Region splitting has long been considered but only recently become wider spread in creep modelling [51]:

> *'According to the concept of the deformation and fracture mechanisms map we should accept the assumption that creep rupture data attained within the domain where creep or creep fracture is governed by one dominant mechanism cannot be used for prediction to another domain, where creep and fracture are controlled by different dominant mechanisms. As soon as*

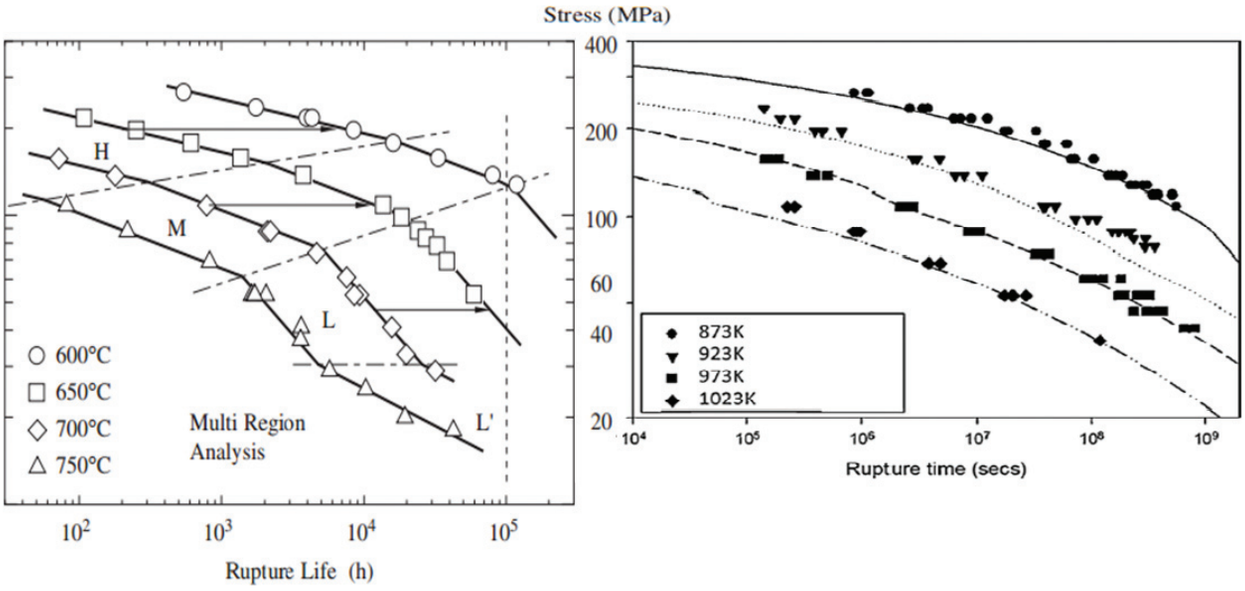

Figure 12. Region splitting by Maruyama et al. for 316 stainless steel [53] (left), and, Wilshire et al. for 316H stainless steel [49] (right).

> *the condition is changed and the boundary is crossed into another domain, the prediction becomes unreliable' [52].*

Therefore region splitting is the segmenting of creep data according to dominant creep mechanism.

For power-law models of creep, region splitting has two major implementations. The first method of implementing region splitting is to fit a model and use linear regression to define regions. For 316 steel shown in **Figure 12**, it can be seen that this approach implemented by Maruyama et al. [53] results in multiple regions not associated with specific microstructural mechanism changes. The alternate power-law approach used by Kimura et al. [54] is to region split at ~0.5$\sigma_{0.2\%PS}$ which for most steels coincides with the elastic limit of the material. Kimura et al. use the same activation energy across both regions and using the stress exponent, n, to reflect the mechanism change. Both these power-law approaches to region splitting are problematic. The first essentially reduces the dataset to obtain the best model fit regardless of creep mechanism and would prove difficult to independently reproduce. The second method uses a known material property limit to split data but does not have the flexibility to apply to different materials such as superalloys, and furthermore to multiple regions as seen in Grade 22, 23, and 24 [47].

When used in conjunction with the Wilshire equations region splitting becomes significantly more consistent and reproducible. Throughout the examples in this chapter, region splitting for the Wilshire equations has been implemented through the change constants k_u, u, k_v and v, as well as, the change in activation energies Q_c*. In each case, these changes in constants have

coincided with changes in creep mechanism, with microstructural evidence provided. Furthermore, these regions have not been determined subjectively but rather as a result of the implementation of the Wilshire equations.

Furthering research into modelling creep over wider ranges of stress and temperature, region splitting is becoming more important in characterising the behaviour seen. Power-law approaches region split either by regression or through selecting a material property limit associated with a change in creep mechanism. This is problematic as it is not linked to the underlying mechanisms, or, is predefined and unable to model multiple regions. The Wilshire equations throughout this chapter have implemented region splitting producing better long-term predictions and regions that reflect changes in actual creep mechanisms.

5. Conclusion

The power-law governing creep behaviour is an empirical relationship that inherently assumes a transition from diffusion to dislocation driven creep. This relationship uses a combination of stress exponent, n, and activation energy, Q_c, to determine the underlying creep mechanism which often do not agree, and do not describe the actual dominant creep mechanism. As an alternate approach the Wilshire Equations were developed.

In a fair comparison to the power-law for polycrystalline copper, the Wilshire Equations reflected the change in creep curve shape seen at the yield stress. The power-law did not indicate any change in creep behaviour then proceeded to 'power-law breakdown'.

In developing a creep modelling technique, confidence in extrapolation is critical. For 9–12% Cr Steels Grade 91, 92 and 122, it was shown that data from tests <5000 h in duration was able to predict 100,000 h creep strengths. Furthermore, the Wilshire equations again reflected a change in creep behaviour with Grade 92 and 122 having 2 regions with Grade 91 only having 1. This mirrored changes in the Reduction of Area and ductility of the tests with Grade 91 behaving differently to Grades 92 and 122. Further development of the equations in the 2.25Cr series of alloys revealed the requirement of a non-constant activation energy, which it is argued more closely represents the observed micromechanical behaviour observed in a range of materials.

Support for this argument was achieved through the application of the Wilshire approach to Waspaloy where a change in creep mechanism around the yield stress was clearly observed. Through TEM observations, below yield dislocation interactions with γ' particles were identified as the primary hardening mechanism, whereas above yield forest hardening was identified leading to the distance between dislocations becoming the critical factor.

The evidence therefore supports the Wilshire Equations satisfying 3 critical criteria, firstly to reflect changing creep behaviour, secondly to be able to extrapolate to long lives, and, finally to reflect the underlying physical process of the creep mechanism. In achieving this it is recognised that the Wilshire Equations provide a significant step forward in creating accurate methods of analysis and long-term prediction based on the underlying physics and creep mechanisms.

Author details

Mark Whittaker*, Veronica Gray and William Harrison

*Address all correspondence to: m.t.whittaker@swansea.ac.uk

Institute of Structural Materials, College of Engineering, Swansea University, UK

References

[1] Boyce MP. Gas Turbine Engineering Handbook. 2nd ed. Woburn, MA: Gulf Professional Publishing; 2002. 816 p

[2] British Standard A23(5); 1948

[3] British Standard 1686(6); 1950

[4] British Standard 1687(7); 1950

[5] British Standard 1688(8); 1950

[6] Monkman FC, Grant NJ. An empirical relationship between rupture life and minimum creep rate. In: Grant NJ, Mullendore AW, editors. Deformation and Fracture at Elevated Temperatures. Boston: MIT Press; 1965

[7] Norton FH. The Creep of Steels at High Temperatures. New York: McGraw-Hill; 1929. 112 p

[8] Arrhenius SA. Über die Dissociationswärme und den Einfluß der Temperatur auf den Dissociationsgrad der Elektrolyte. Zeitschrift für Physikalische Chemie. 1889;**4**:96-116

[9] Wilshire B, Whittaker MT. The role of grain boundaries in creep strain accumulation. Acta Materialia. 2009;**57**(14):4115-4124

[10] Cadek J, Zhu SJ, Milicka K. Threshold creep behaviour of aluminium dispersion strengthened by fine alumina particles. Materials Science and Engineering A. 1998;**252**:1-5

[11] Zhu H, Seo DY, Maruyama K, Au P. Effect of microstructural stability on creep behaviour of 47XD TiAl alloys with fine-grained fully lamellar structure. Scripta Materialia. 2005; **52**:45-50

[12] Sato H, Fujita K. Quantification of creep rate changes and life prediction by means of strain-accelerated-parameter. Keikinzoku. 2010;**60**(7):353-357

[13] Wilshire B, Sharning PJ. A new methodology for analysis of creep and creep fracture data for 9-12% chromium steels. International Materials Reviews. 2008;**53**(2):91-104

[14] Weertman J. Theory of steady-state creep based on dislocation climb. Journal of Applied Physics. 1955;**26**:1213

[15] Weertman J. Steady-state creep through dislocation climb. Journal of Applied Physics. 1957;**28**:362

[16] Glen JW. The creep of polycrystalline ice. Proceedings of the Royal Society A. 1955;**228**(1175): 519-538

[17] Glen JW. Rate flow of polycrystalline ice. Letters to Nature. 1953;**172**:721-722

[18] Nye JF. The flow of ice from measurements in glacier tunnels, laboratory experiments and the Jungfraufirn borehole experiment. Proceedings of the Royal Society A. 1139;**219**:1953

[19] Kassner WE, Pérez-Prado M-T. Five-power-law creep in single phase metals and alloys. Progress in Materials Science. 2000;**45**(1):1-102

[20] NIMS Japan. Creep Data Sheet No: 51; 2006

[21] Wilshire B, Sharning PJ. Long-term creep life prediction for a high chromium steel. Scripta Materialia. 2007;**56**(8):701-704

[22] Kimura K, Shibli IA, Holdsworth SR, Merckling G. Creep and Creep Fracture in High Temperature Components-Design and Life Assessment Issues. DEStech: Lancaster, PA; 2005

[23] Maruyama K, Lee JS, Shibli IA, Holdsworth SR, Merckling G. Design and life issues. In: Creep and Creep Fracture in High Temperature Components. Lancaster, PA: DEStech; 2005. pp. 372-379

[24] Wilshire B, Sharning PJ. Rationalization and extrapolation of creep and creep fracture data from grade 91 steel. Materials at High Temperatures. 2008;**25**(2):55-65

[25] Wilshire B, Sharning PJ. A new approach to creep data assessment. Materials Science and Engineering A. 2009;**510**:3-6

[26] Whittaker MT, Wilshire B. Creep and creep fracture of 2.25Cr-1W steels (grade 23). Materials Science and Engineering A. 2010;**527**(18):4932-4938

[27] Larson FR, Miller J. A time-temperature relationship for rupture and creep stresses. Transactions ASM. 1954;**74**:765-775

[28] Orr R, Sherby O, Dorn J. Correlation of rupture data for metals at elevated temperatures. Transaction ASM. 1954;**46**:113-118

[29] Manson S, Succop G. Stress-rupture properties of inconnel 700 and correlation on the basis of several time-temperature parameters. ASTM Special Publication. 1956;**174**:40

[30] Manson S, Haferd A. A linear time-temperature relation for extrapolation of creep and stress-rupture data. NASA Technical Note 2890. 1953

[31] Goldhoff R, Hahn G. Correlation and extrapolation of creep-rupture data of several steels and superalloys using time-temperature parameters. ASM Publication. 1968;**D-8-100**:199-247

[32] Abdullah Z, Gray V, Whittaker MT, Perkins KM. A critical analysis of the conventionally employed creep lifing methods. Materials. 2014;**7**(5):3371-3398

[33] Gray V, Abdullah Z, Whittaker MT. Determining the Parameters and Constants of Failure. Swansea University, Berlin, Germany: ResearchGate; 2015. DOI: 10.13140/RG.2.1.3639.9520

[34] Gibbs GB. The thermodynamics of creep deformation. Physica Status Solidi B. 1964; **5**(3):693-696

[35] Wilshire B, Sharning PJ. A new methodology for analysis of creep and creep fracture data for 9-12% chromium steels. International Materials Review. 2008;**53**(2):91-104

[36] Wilshire B, Battenbough AJ. Creep and fracture of polycrystalline copper. Materials Science and Engineering A. 2007;**443**:156-166

[37] Burton B, Greenwood GW. The limit of the linear relation between stress and strain rate in the creep of copper and copper-zinc alloys. Acta Metallurgica. 1970;**18**(12): 1237-1242

[38] Feltham P, Meakin JD. Creep in face-centred cubic metals with special reference to copper. Acta Metallurgica. 1959;**7**(9):614-627

[39] Burton B, Greenwood GW. The contribution of grain-boundary diffusion to creep at low stresses. Metal Science Journal. 1970;**4**(1):215-218

[40] Evans RW, Wilshire B. Creep of Metals and Alloys. London, UK: Institute of Metals; 1985. p. 314

[41] Holdsworth SR, Bullough CK, Orr J. BS PD 6605 creep rupture data assessment procedure. ECCC Recommendations. 2001

[42] NIMS Creep Data Sheet No. 43; 1996

[43] NIMS Creep Data Sheet No. 48; 2002

[44] NIMS Creep Data Sheet No. 51; 2006

[45] Arzt E. Creep of dispersion strengthened materials: A critical assessment. Mechanics Research. 1991;**31**:399-453

[46] Kimura K. Present status and future prospect on NIMS creep data sheet. In: Mishra RS, Earthman JC, Raj SV, editors. Creep Deformation and Fracture, Design and Life Extension. Pittsburgh: MS&T; 2005. pp. 97-106

[47] Whittaker MT, Wilshire B. Advanced procedures for long-term creep data prediction for 2.25 chromium steels. Metallurigcal and Materials Transactions A. 2013;**44**:136-153

[48] Whittaker MT, Harrison WJ. Evolution of the Wilshire equations for creep life prediction. Materials at High Temperatures. 2014;**31**(3):233-238

[49] Evans M, Whittaker MT, Wilshire B. Long-term creep data prediction for type 316H stainless steel. Materials Science and Engineering A. 2012;**552**:145-150

[50] Whittaker MT, Harrison WJ, Deen C, Rae C, Williams S. Creep deformation by dislocation movement in Waspaloy. Materials. 2017;**10**:61

[51] Gray V, Whittaker MT. The changing constant of creep: A letter on region splitting in creep lifing. Materials Science and Engineering A. 2015:**632**:96-102

[52] Foldyna V, Kubon Z, Jakobova A, Vodarek V. Development of advanced high chromium Ferritic steels. In: Microstructural Development and Stability in High Chromium Ferritic Power Plant Steels. London, UK: The Institute of Materials; 1997. pp. 73-92

[53] Maruyama K, Ghassemi Armaki H, Yoshimi K. Multiregion analysis of creep rupture data of 316 stainless steel. International Journal of Pressure Vessels and Piping. 2007;**84**(3):717

[54] Kimura K. Creep rupture strength evaluation with region splitting by half yield. Proceedings of the ASME 2013 Pressure Vessels & Piping Division Conference. 2013